A more complete record of sample preparation for reaction with CaH_2 is provided below:

Two different methods were used to prepare $SrTiO_3$ samples for hydride doping via reaction with CaH_2. For the first round of synthesis, $SrTiO_3$ crystals were pressed into pellets of CaH_2 powder to ensure close surface contact and facilitate ion exchange. Singly polished, 0.5 x 10 x 10 mm crystal substrates of $SrTiO_3$ from MSE Supplies® (>99.9% purity, (100) orientation) were sliced into roughly 2.5 x 2.5 mm squares using a wire saw. These crystal slices were dried overnight in a 150° C desiccator oven to ensure no H_2O surface contamination. All subsequent sample preparation then took place in an Ar glovebox to further avoid contamination. A granular CaH_2 powder purchased from Thermo Scientific Chemicals (98% metal basis purity) was ground in an alumina mortar and pestle for 15 minutes in preparation for pressing into pellets. Crystal slices were immersed in the finely ground CaH_2 powder in a 7 mm pellet die and pressed to 1.5 tons using a Specac hydraulic press. A molar excess of CaH_2 (~165 mg) was used for each pellet. Two pellets each were placed into 9 mm fused silica tubes, which were then evacuated to 0.01 Pa and sealed using a gas-oxygen torch at a total tube length of ~30 cm.

Sample tubes were placed directly into a tube furnace preheated to the final reaction temperature (600, 700, or 800 °C). All tubes being treated at the same temperature were placed into the furnace at the same time, and two tubes were designated for each treatment time in the sample series (four pellets per temperature-time condition). At the end of a synthesis run, sample tubes were removed from the furnace and plunged into liquid nitrogen. The crystals were recovered by dissolving the CaH_2 pellets in a mixture of isopropyl alcohol and deionized water (~3:1 ratio). The recovered crystals were sonicated in deionized water to remove unwanted reaction products from their surfaces.

Because these pelletized samples were deformed, cracked or shattered either upon recovery or during preparation, a second round of syntheses was carried out to produce samples suitable for transmission spectroscopy (i.e., FTIR and UV-vis). In this round of synthesis, the $SrTiO_3$ substrates were sliced into ~3.3 x 10 mm slices using a wire saw. A secondary 4 mm ID fused silica tube ~5 cm long was packed with CaH_2 powder, and the $SrTiO_3$ crystal slices were immersed in the powder. These secondary tubes were then placed into the bottoms of longer 9 mm tubes and sealed in the same manner as the pelletized samples. The procedure for treatment in the furnace was identical to the pelletized samples, except the tubes were allowed to cool to room temperature in air, rather than being plunged in liquid nitrogen. One sample (SC-70048h) was treated in this manner through two separate 24-hour steps.

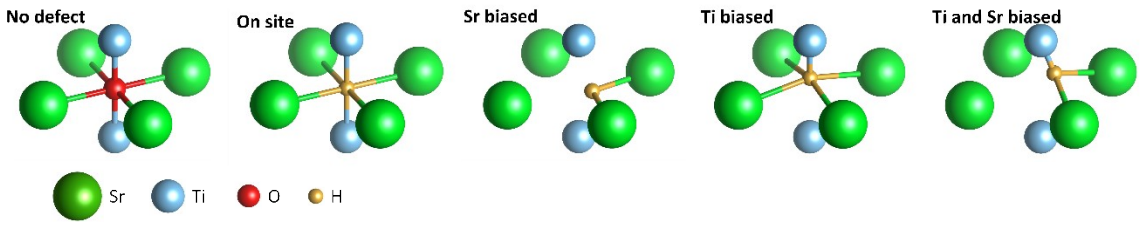

Figure S.1 *– The possible occupations of an oxygen vacancy by a single hydride ion tested via DFT. Of these four, only the direct on-site occupation was found to be stable in all supercell sizes. The Sr-biased, off-site occupation was found to be stable only in the 2x2x2 supercell, where it was favored by 25 meV.*

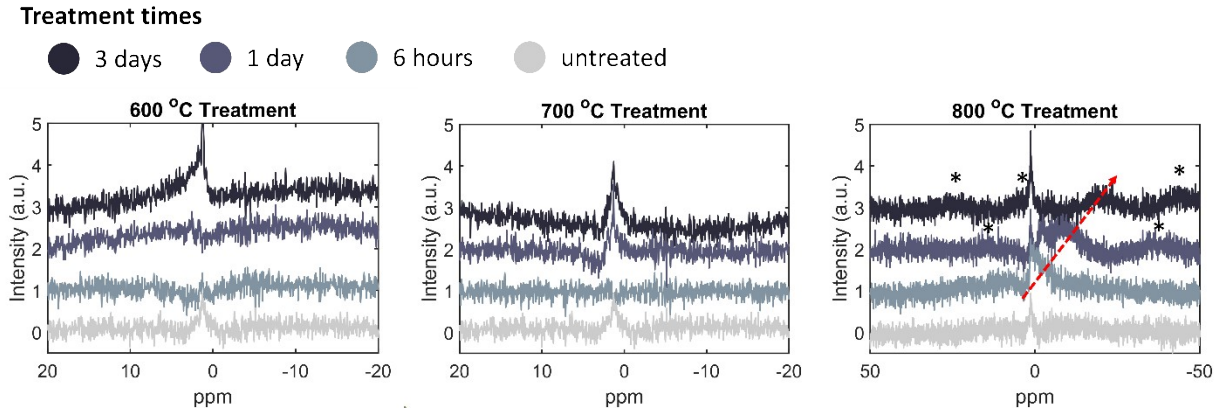

Figure S.2 *– ^{1}H MAS NMR spectra (spinning speed of 12000 Hz) from the initial run of pellet-prepared samples, plotted against the spectrum from untreated $SrTiO_3$. All samples were mixed with fused quartz powder. For syntheses carried out at 600 and 700 °C, there is no discernable signal associated with structural H^-, but rather sharp features located near 1 ppm that are likely due to adsorbed water. The samples treated at 800 °C also contain these features, but also have the broad, negative shifted peaks associated with hydride (note the extended data range compared to the other two plots). Progressive treatment increases the magnitude of the negative shift, as indicated by the red arrow. For the samples treated for 1 day, multiple features might be present, possibly due to the fact that these samples consist of 4 separate crystals that may vary slightly in hydride content. Spinning sidebands of ^{1}H MAS NMR signal are marked with *.*

Calculation	Ti-H-Ti stretch position (cm^{-1})
Finite differences, 2×2×2 cell	1307.7
Finite differences, 3×2×2 cell	1301.0
Finite differences, 3×3×2 cell	1304.7
Finite differences, 3×3×3 cell	1342.1
Perturbation theory, 3×3×2 cell	1327.5

Table 5.2 *– Summary of mode positions predicted by 0 K methods.*

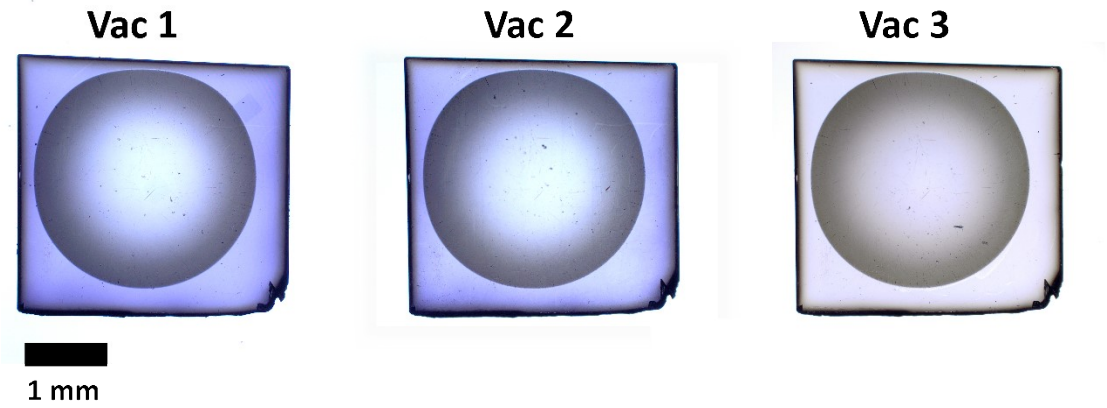

Figure S.3 *– Images of the vacuum treated sample with a dimple ground into the center. This sample material was sliced from SC-70048h. Stage 1 was a 3.5 hr vacuum anneal at 500 °C, stage 2 was an additional 3.5 hr, 500 °C anneal, and stage 3 was a 3.5 hr vacuum anneal at 600 °C. Over the course of treatments, the crystal transitioned to a more transparent, purple state, lost color, and then became completely colorless.*

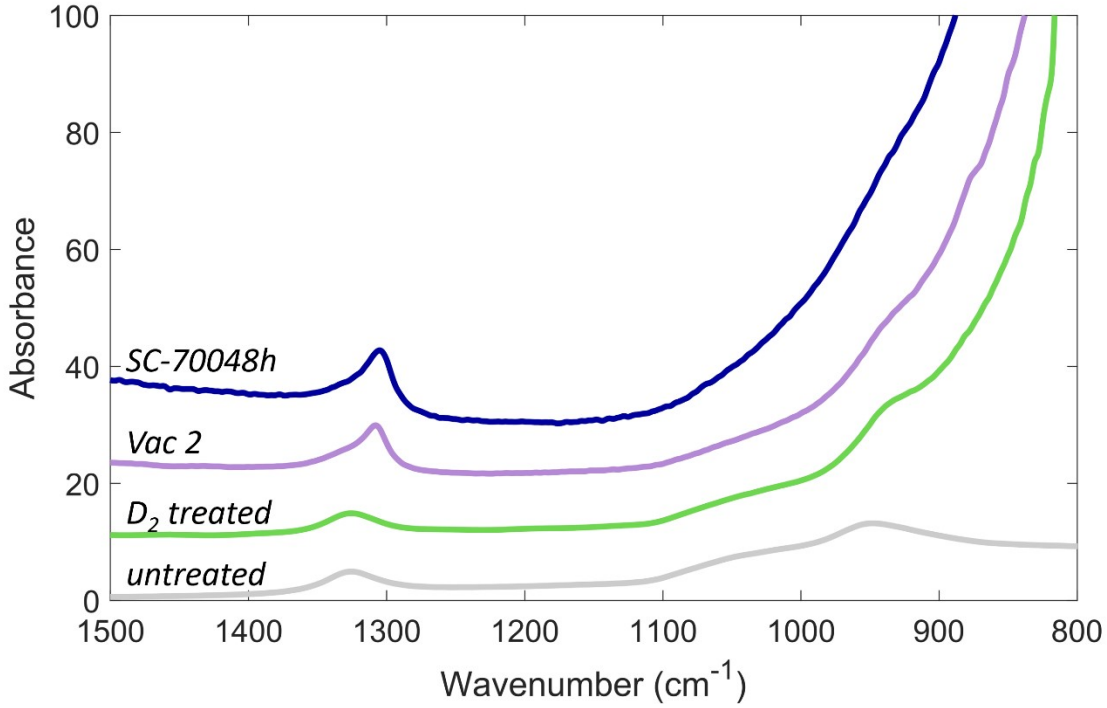

Figure S.4 *– Comparison between infrared spectra of different samples showing the dramatic differences that occur below 1000 cm^{-1}. All spectra are scaled to 1 cm path length. In the case of the untreated sample, features below 950 cm^{-1} are truncated in a way that gives the illusion of on-scale absorbance. For sample SC-70048h, the edge of the intense features centered somewhere below 800 cm^{-1} occurs a few hundred cm^{-1} higher than expected. This effect can also be seen to a lesser extent in the spectrum from sample Vac2. In the D_2-treated sample, it's possible that these effects are at play in the ~920 cm^{-1} region, where Ti-D-Ti stretching modes are expected to reside. The feature centered around 940 cm^{-1} in the D_2-treated sample is most likely native to $SrTiO_3$, rather than being deuterium-related, as it also occurs in Vac 2 and SC-70048h. However, the shape and apparent intensity across samples are distorted by the effects described above.*

Raman spectroscopy

Samples prepared via the capsule method were also analyzed via Raman spectroscopy. The Raman spectra show that while all samples are still $SrTiO_3$, there are some departures from the spectra of untreated $SrTiO_3$ crystals. We find that CaH_2 treatment results in the emergence of modes located at 128 cm^{-1}, 480 cm^{-1}, 693 cm^{-1}, and 803 cm^{-1}, with the 693 cm^{-1} being the most prominent. Additionally, the broad mode centered at ~300 cm^{-1} progressively decreases with more intense treatment. We attribute these modes to distortions of the $SrTiO_3$ structure resulting from H^- incorporation. Local distortions could cause subtle changes in cation site geometry and thus new Raman active modes. The extremely high symmetry of the pristine $SrTiO_3$ structure (single cubic perovskite) could make it especially susceptible to such affects. Despite the abundant new Raman-active modes, we find that there is no emergent polarization behavior, suggesting that the $SrTiO_3$ crystals are still isotropic and H^- incorporation has not pushed them into tetragonal or orthorhombic phase space, akin to the $BaTiO_3$ or $CaTiO_3$ structures.

Interestingly, when higher laser powers are used and exposure time to the laser is increased, the intensities of these features subside. Upon reduced exposure to the laser, these spectra then slowly return to their original states. There could be several reasons for this behavior. One possibility we propose is that the laser heats the samples, perhaps temporarily relaxing some of the local site distortion, reverting back to a higher symmetry state. It is important to note that none of the emergent features we observe appear to be equivalent to any of the predicted H-associated normal modes. Although there may be some Raman activity associated with certain hydride modes, our samples likely do not contain high enough concentrations of H^- to produce features detectable via Raman spectroscopy. Notably, these emergent Raman features are absent from other published Raman spectra of $SrTiO_3$ crystals, including those annealed under H_2[1].

1 S. Mochizuki, F. Fujishiro, K. Ishiwata and K. Shibata, *Physica B: Condensed Matter*, 2006, **376–377**, 816–819.

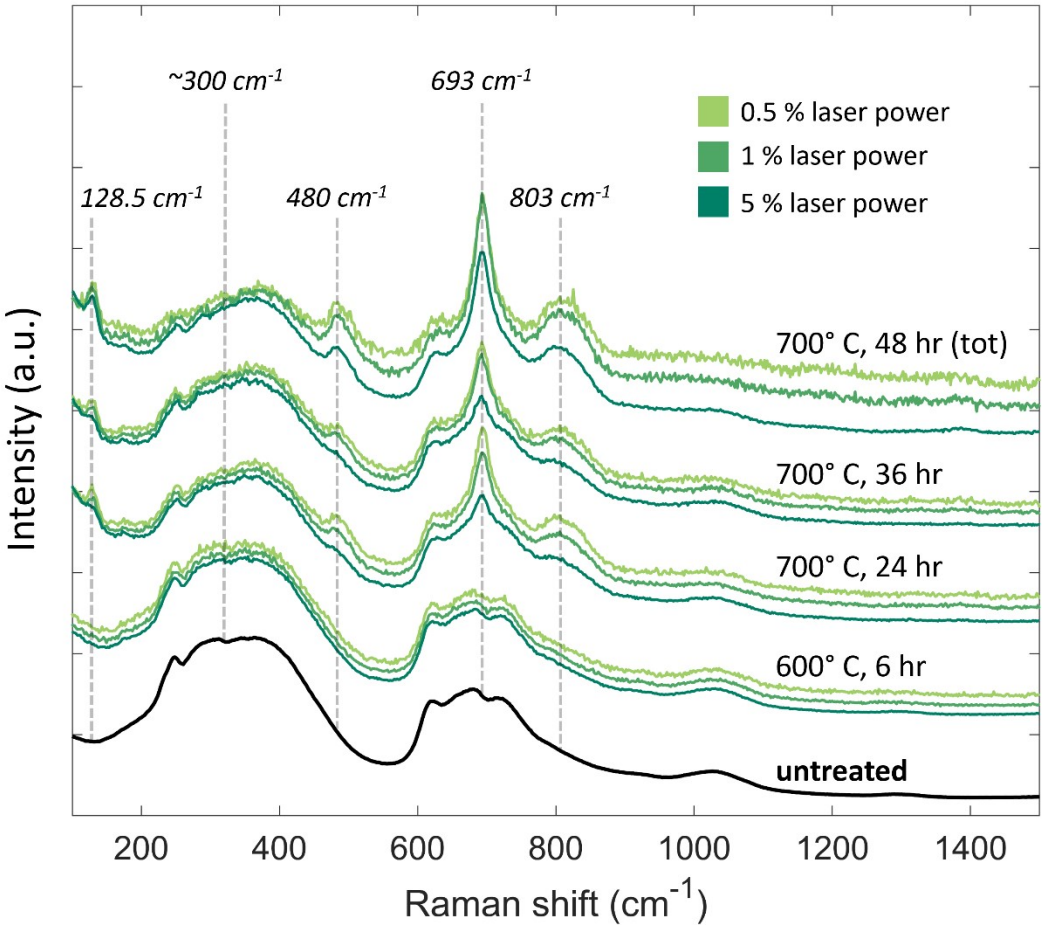

Figure S.5 *–Raman spectra of the capsule-treated samples. Increased treatment conditions result in an increase in feature intensities at 128.5 cm^{-1}, 480 cm^{-1}, 693 cm^{-1}, and 803 cm^{-1}. Increasing the Raman laser power resulted in a decrease in the intensities of these features. A broad mode located at approximately 300 cm^{-1} decreases in intensity with increasing hydride content.*